Inorganic Chemistry

Article

pubs.acs.org/IC

Copper Phosphonatoethanesulfonates: Temperature Dependent in Situ Energy Dispersive X-ray Diffraction Study and Influence of the pH on the Crystal Structures

Mark Feyand,[†] Annika Hübner,[†] André Rothkirch,[‡] David S. Wragg,[§] and Norbert Stock*,[†]

[†]Institut für Anorganische Chemie, Christian-Albrechts-Universität, Max-Eyth Straße 2, D 24118 Kiel, Germany

[‡]HASYLAB, DESY Hamburg, Notkestraße 85, 22607 Hamburg, Germany

[§]Centre for Materials Science and Nanotechnology/InGAP/Department of Chemistry, University of Oslo, Postbox 1033, Blindern, 0315 Oslo, Norway

Supporting Information

ABSTRACT: The system $Cu^{2+}/H_2O_3P-C_2H_4-SO_3H$/NaOH was investigated using in situ energy dispersive X-ray diffraction (EDXRD) to study the formation and temperature induced phase transformation of previously described copper phosphonosulfonates. Thus, the formation of $[Cu_2(O_3P-C_2H_4-SO_3)(OH)(H_2O)]\cdot 3H_2O$ (**4**) at 90 °C is shown to proceed via a previously unknown intermediate $[Cu_2(O_3P-C_2H_4-SO_3)(OH)(H_2O)]\cdot 4H_2O$ (**6**), which could be structurally characterized from high resolution powder diffraction data. Increase of the reaction temperature to 150 °C led to a rapid phase transformation to $[Cu_2(O_3P-C_2H_4-SO_3)(OH)(H_2O)]\cdot H_2O$ (**1**), which was also studied by in situ EDXRD. The comparison of the structures of **1**, **4**, and **6** allowed us to establish a possible reaction mechanism. In addition to the in situ crystallization studies, microwave assisted heating for the synthesis of the copper phosphonosulfonates was employed, which allowed the growth of larger crystals of $[NaCu(O_3P-C_2H_4-SO_3)(H_2O)_2]$ (**5**) suitable for single crystal X-ray diffraction. Through the combination of force field calculations and Rietveld refinement we were able to determine the crystal structure of $[Cu_{1.5}(O_3P-C_2H_4-SO_3)]\ 2H_2O$ (**3**) and thus structurally characterize all compounds known up to now in this well investigated system. With the additional structural data we are now able to describe the influence of the pH on the structure formation.

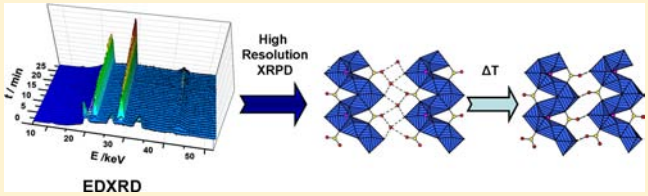

INTRODUCTION

Inorganic−organic hybrid compounds are presently of great interest because of their potential prospects in gas storage, catalysis, and as nanoscale carriers for medical applications.[1−3] Most of these compounds are based on polycarboxylates,[4] -phosphonates,[5−7] or -sulfonates.[8] Inorganic−organic hybrid compounds based on polyfunctionalized linker molecules show a large structural variety depending on the reaction conditions such as reaction temperature and molar ratios of the starting materials.[9−15] In the past polyfunctionalized, phosphonate-based organic building units such as phosphonocarboxylates,[16] phosphonosulfonates,[13,17−20] or aminophosphonates[21−24] were investigated. Most of these compounds were obtained by crystallization from solutions or under solvothermal conditions, and these sealed reaction conditions make obtaining information about crystallization difficult. In principle numerous methods are available that allow study of the crystal formation,[25] but only a few studies dealing with the formation of inorganic−organic hybrid compounds have been reported. Among these, in situ EXAFS,[26] AFM,[27] in situ light scattering,[28,29] in situ neutron diffraction,[30] and in situ energy dispersive X-ray diffraction (EDXRD)[17,31−35] studies have been carried out.

In situ EDXRD has proven to be a valuable tool to investigate crystallization. In the past intercalation reactions,[36,37] the crystallization of thioantimonates,[37] metal oxides,[38] metal−organic frameworks (MOFs)[31,32,34] and the structural flexibility of MOFs[39] were investigated. There are only three studies up to now that have focused on the crystallization of metal phosphonates using EDXRD methods.[17,40] In EDXRD studies extremely intense white beam synchrotron radiation is employed to achieve a good time resolution (less than a minute) while using conventional reaction vessels in the experiments. The white beam is sufficiently intense to penetrate steel autoclaves and thus reactions can be investigated without imposing an external influence on the reaction mixture if no beam sensitive solvents are used.[41] In addition no scanning in 2θ is needed because of the fixed angle of the solid state detector. EDXRD experiments allow to extract kinetic parameters such as rate constants, Arrhenius activation energies, or to determine possible reaction mechanisms.[17,37,42] In addition to quantitative analyses, it is possible to observe crystalline intermediates which may not be accessible by quenching or ex situ studies.[17,31] Such

Received: September 10, 2012
Published: November 9, 2012

   dx.doi.org/10.1021/ic301976s | *Inorg. Chem.* 2012, 51, 12540−12547

intermediates can give new insights into the crystallization process or even help to establish a possible reaction mechanism.[37]

We are interested in the synthesis of inorganic−organic hybrid compounds based on polyfunctionalized linker molecules. Previously we have carried out a study of the reaction system $Cu^{2+}/H_2O_3P-C_2H_4-SO_3H/NaOH$ in water in the temperature range of 90 to 190 °C using high throughput methods.[43,44] The systematic study allowed us to establish the fields of formation of five new hybrid compounds which are mainly defined by the reaction temperature range and the pH range of the reaction mixture (Figure 1). Structural trends

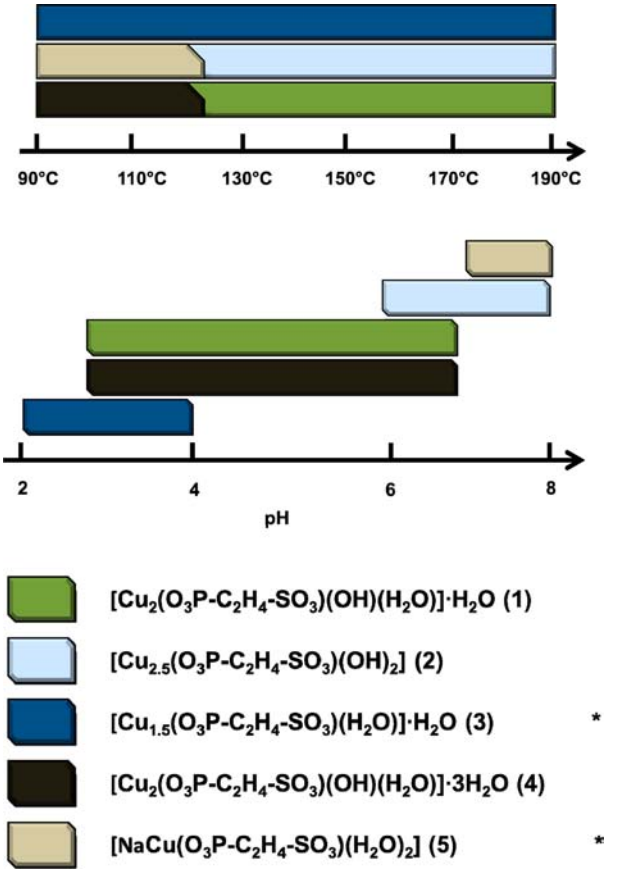

Figure 1. Reaction trends in the system $Cu^{2+}/H_2O_3P-C_2H_4-SO_3H/NaOH$ in water.[43] The structures of **3** and **5** (marked with *) are reported in this study.

could only be established for the phases formed at elevated temperatures ($[Cu_2(O_3P-C_2H_4-SO_3)(OH)(H_2O)]\cdot H_2O$ (**1**), $Cu_{2.5}(O_3P-C_2H_4-SO_3)(OH)_2$ (**2**), $[Cu_2(O_3P-C_2H_4-SO_3)(H_2O)_2(OH)]\cdot 3H_2O$ (**4**)) which were structurally characterized.[43,45]

Here we report the results of our in situ EDXRD study of the system $Cu^{2+}/H_2O_3P-C_2H_4-SO_3H/NaOH$ to investigate the temperature dependent formation of copper phosphonatosulfonates. Furthermore, the influence of microwave assisted heating and the use of force field calculations in conjunction with Rietveld methods for the structure elucidation are presented. These approaches resulted in three new crystal structures and a reaction mechanism, and the synthesis-structure relationship of the whole system was established as well.

EXPERIMENTAL SECTION

4-Phosphonoethanesulfonic acid (H_3L) was synthesized in the literature in a two-step nucleophile substitution reaction starting from 1,2-dibromoethane and using triethylphosphite and sodium sulfite, as previously reported.[9] All other reagents were of analytical grade (Fluka and Aldrich) and were used without further purification. XRPD measurements were carried out on a Stoe Stadi P diffractometer in transmission geometry with Cu−$K_{\alpha 1}$ radiation, equipped with an image plate detector system or a linear PSD detector system for high resolution data. The MIR spectra were recorded on a Bruker ALPHA-P FT-IR spectrometer in the spectral range 4000−400 cm^{-1}. For the thermogravimetric analyses under air a NETSCH STA 409 CD analyzer was used with a heating rate of 4 K/min and an air flow rate of 75 mL/min. Electron microscopy and EDX analysis were carried out on a Phillips XL ESEM. High resolution powder XRD patterns were measured at beamline G3 at HASYLAB, DESY, Hamburg.[46] Single crystal measurement was carried out on a Bruker D8 3-circle diffractometer with an Apex II CCD detector. Syntheses were carried out under solvothermal conditions DURAN culture tubes 12 × 100 mm D50 GL 14 M.KAP, SCHOTT 261351155 for conventional heating, and an Anton Paar Synthos 3000 high-throughput microwave reactor system with custom-made Teflon inserts for microwave assisted heating.

In Situ Crystallization Experiments. EDXRD experiments were carried out at HASYLAB, beamline F3 at DESY, Hamburg, Germany. The white beam synchrotron radiation (4 to 55 keV) was detected by a liquid nitrogen cooled germanium semiconductor detector system. The detector angle was set to approximately 1.9°. The best results were obtained by collimating the beam to 0.2 × 0.2 mm^2. To heat the samples a custom-made reactor system heated by an external thermostat (JULABO) was used. The reaction temperature of the reaction mixture is achieved within 2 min.[42]

In Situ EDXRD Study of $[Cu_2(O_3P-C_2H_4-SO_3)(H_2O)_2(OH)]\cdot 3H_2O$ (4). The in situ experiments were carried out in Duran glass reactors. 2.0 M H_3L (263 μL, 0.53 mmol), 2.0 M $Cu(NO_3)_2$ (536 μL, 1.06 mmol), and 2.0 M NaOH (789 μL, 1.59 mmol) were combined, and H_2O was added to give the final volume (2500 μL).[43] The mixture was homogenized by shaking before transferring the vessel in the in situ reactor system. The reaction was carried out at 90 °C.

In Situ Transformation of 4 to $[Cu_2(O_3P-C_2H_4-SO_3)(H_2O)_2(OH)]\cdot H_2O$ (1).[43] The reaction mixture of the in situ experiment for the synthesis of **4** was temporarily removed from the in situ reactor. The reactor temperature was increased to 150 °C and the sample was reinserted into the in situ reactor.

Quenching Experiments of $[Cu_2(O_3P-C_2H_4-SO_3)(H_2O)_2(OH)]\cdot 4H_2O$ (6). 2.0 M H_3L (263 μL, 0.53 mmol), 2.0 M $Cu(NO_3)_2$ (536 μL, 1.06 mmol), and 2.0 M NaOH (789 μL, 1.59 mmol) were combined in a glass vessel and H_2O was added to give the final volume (2500 μL). The reaction mixture was stirred for 10 min at room temperature and the slightly blue solid was filtered and washed with water and immediately used for characterization.

Synthesis of $[Cu_{1.5}(O_3P-C_2H_4-SO_3)]\cdot 2H_2O$ (3). Twenty-six microliters of a 2 M H_3L, 79 μL H_2O, 79 μL of a 2 M $Cu(NO_3)_2$ solution, and 26 μL of a 2 M NaOH were added to a high-throughput Teflon reactor with a total volume of 250 μL.[44] The Teflon reactor was placed in a high-throughput steel reactor, sealed, and heated up in 6 h to 110 °C. The temperature was held for 48 h, and the reaction mixture was cooled down to room temperature in 6 h. The light blue product was filtered and washed with water. Larger amounts of the product were obtained by using five times the amount in a high-throughput reactor with a total volume of 2 mL (yield 77% and 89% based on H_3L).

Microwave-Assisted Synthesis of $NaCu(O_3P-C_2H_4-SO_3)(H_2O)_2$ (5). Suitable single crystals of **5** were obtained by mixing 132 μL of a 2 M H_3L solution, 258 μL H_2O, 105 μL of a 2 M $Cu(NO_3)_2$ solution, and 105 μL of a 2 M NaOH solution in a 4 mL subsuming high-throughput Teflon reactor. The reaction mixture was heated for 6 h in an Anton Paar Synthos 3000 high-throughput microwave reactor. The product was filtered off and washed with

dx.doi.org/10.1021/ic301976s | Inorg. Chem. 2012, 51, 12540−12547

water. A mixture of blue plates (50−80 μm) and small amounts of a light blue powder were obtained.

Structure Determination. All crystal data, and structure refinement parameters of compound **3**, **5**, and **6** are summarized in Table 1.

Table 1. Summary of the Important Crystallographic Parameters of the Structure Determination and Refinement

	$[Cu_2(O_3P-C_2H_4-SO_3)(H_2O)_2(OH)]\cdot 4H_2O$ (**6**)	$[Cu_{1.5}(O_3P-C_2H_4-SO)(H_2O)_2]$ (**3**)	$[NaCu(O_3P-C_2H_4-SO_3)(H_2O)_2]$ (**5**)
structure determined from	powder data	powder data	single crystal data
formula sum	$Cu_2C_2O_{13}PS$	$Cu_{1.5}C_2SPO_8$	$CuC_2H_8NaPSO_8$
Z	4	2	4
crystal system	monoclinic	triclinic	monoclinic
a/Å	13.754(4)	5.0944(1)	14.757(3)
b/Å	7.1015(2)	8.4853(1)	7.690(1)
c/Å	13.491(4)	10.5077(2)	7.481(2)
α/deg	90	111.99(1)	90
β/deg	104.72(3)	93.07(1)	92.41(3)
γ/deg	90	101.29(1)	90
V/Å^3	1274.5(6)	408.9(1)	848.3(3)
space group	$P2_1/n$	$P\bar{1}$	$P2_1/c$
solution method	direct methods, Expo2009[47]	force field calculation, Materials Studio 5.3[48]	direct methods ShelXS[49]
refinement method	least-squares Rietveld[50]	least-squares Rietveld[50]	least-squares ShelXL[49]
R_{wp}, R_{Bragg}	0.088, 0.034	0.085, 0.021	
R_{wp}/R_{exp}	5.29	1.39	
GOF			0.89
tot., uniq. data, R_{int}			7170, 2073, 0.094
Observed data [$I > 2\sigma(I)$]			1693
R1, wR2			0.0405, 0.1288
Δe min./max. (e/Å^3)			−1.15, 1.92

Crystal Structure Determination of $Cu_2[(O_3P-C_2H_4-SO_3)(H_2O)_2(OH)]\cdot 4H_2O$ (6). The crystal structure of **6** was determined from high resolution powder diffraction data at beamline G3, HASYLAB, DESY. The sample was mounted in a 0.5 mm quartz capillary. The wavelength was set to 1.54296 Å by a double germanium (111) single crystal monochromator and calibrated with a LaB_6 standard. The diffracted beam was detected by a scintillation counter mounted behind a Soller slit system. The powder pattern was indexed and refined using Topas academics[50] (a = 13.482(1), b = 7.1077(7), and c = 13.7609(8) Å, β = 104.64(8)°, proposed space group $P2_1/n$, GOF = 27, which is related to the value of M20). The structure was solved by direct methods using EXPO 2009 in the space group $P2_1/n$.[47] The intensities were extracted in a 2θ-range from 7.8° to 70° (resolution 1.339 Å). It was possible to determine positions of the copper−oxygen polyhedra and the organic building unit. It is not possible to differentiate between the hydroxide and the water molecules, but the structure shows the same inorganic building unit as the literature known compound $Cu_2[(O_3P-C_2H_4-SO_3)(H_2O)_2(OH)]\cdot 3H_2O$ (**4**).[43] This model was employed in the Rietveld refinement using TOPAS academic[50] ($7.8° \leq 2\theta \leq 80°$). The profile was fitted using a simple axial model and a Thompson−Cox−Hastings profile function. The capillary absorption was corrected using the model by Sabine et al.[51] Four additional water molecules were located between the layers from the difference Fourier map.

Structure Determination of $[Cu_{1.5}(O_3P-C_2H_4-SO_3)(H_2O)]\cdot H_2O$ (3). The structural model of **3** was obtained from an isoreticular compound by force field calculations using Materials Studio 5.3,[48] and the structure was refined from laboratory X-ray powder diffraction data. The powder pattern was successfully indexed using Topas Academic[50] (a = 5.094(2), b = 8.483(2), c = 10.499(2) Å, α = 115.59(1), β = 66.64(1), γ = 101.30(2)°, GOF = 48). The comparison of the lattice parameters with the ones of the literature known compound $[Cu_{1.5}(O_3P-C_4H_8-SO_3)(H_2O)]\cdot 1.15H_2O$[52] shows that the lattice parameters a and c corresponding to the inorganic layers are very similar (a = 5.094(2)/5.1197(5) Å and c = 10.499(2)/10.800(1) Å for the indexed and the literature known compounds, respectively). The b lattice parameter differs substantially b = 8.483(2)/10.533(1) Å, which correlates with the exchange of a $-C_4H_8-$ by a $-C_2H_4-$ group. Starting from the literature known compound the $-C_4H_8-$ groups were replaced by $-C_2H_4-$ groups using Materials Studio 5.1.[48] The model was geometrically optimized using the universal force field implemented in Materials Studio and constraining the lattice parameters to the parameters obtained by indexing. The model was refined by the Rietveld technique using Topas academic 4.1.[50] The profile was fitted in the range 9−80° (2θ) using a Thompson−Cox−Hastings profile function and a simple axial model. Because of the morphology (Supporting Information, Figure S6), a fourth order spherical harmonics series was used to model the preferred orientation induced by the needle like crystal shape.

Crystal Structure Determination of $[NaCu(O_3P-C_2H_4-SO_3)(H_2O)_2]$ (5). The crystal structure of **5** was solved from single crystal X-ray diffraction data. X-ray diffraction measurements were performed on a Bruker D8 3-circle diffractometer with Apex II CCD detector using Mo Kα radiation (λ = 71.073 pm). A hemisphere of diffraction data was collected, and the data were integrated using the program Saint (Bruker AXS, 2003). The data were scaled, and multiscan adsorption correction was applied using the program SADABS

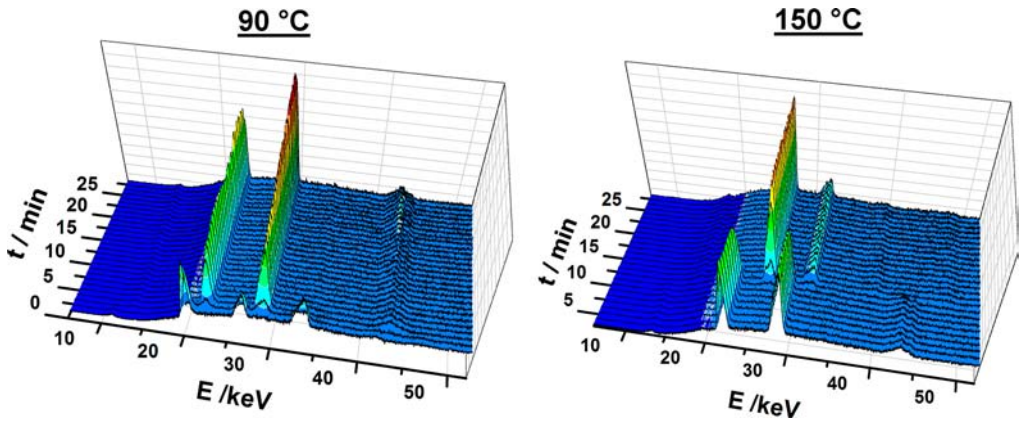

Figure 2. EDXRD spectra series of the crystallization of **4** (left) at 90 °C and its transformation into **1** (right) at 150 °C.

(Bruker (2003). The crystal structures were solved by direct methods with SHELXS-97 and refined using SHELXL-97.[49] H-atoms connected to carbon atoms were placed onto calculated positions. H-atoms of the water molecules were localized in the difference Fourier map and refined as a riding model.

RESULTS AND DISCUSSION

In a previous study of the system $Cu^{2+}/H_2O_3P-C_2H_4-SO_3H$/NaOH the field of formation of five new hybrid compounds had been obtained that allowed extraction of trends regarding temperature and pH dependence (Figure 1).[43] On the basis of the structural data of only three out of five hybrid compounds which were obtained at higher reaction temperatures (130 to 190 °C), we could establish synthesis-structure relationships. Thus, we were able to show that the degree of condensation of the inorganic building unit increases and the number of coordinating and noncoordinating water molecules decreases with increasing temperature.

The extended investigation of the system led to the following results: By using in situ EDXRD measurements, we were able to detect and characterize a previously unknown intermediate that transforms into **4** which itself transforms into **1** upon change of temperature. On the basis of these structures a possible reaction mechanism was deduced. In addition, microwave-assisted synthesis and force field calculations in conjunction with Rietveld methods for the structure elucidation allowed us to structurally characterize all known compounds in the investigated pH and temperature range.

Temperature Dependent In Situ EDXRD Investigation. The crystallization of **4** was investigated at 90 °C. The EDXRD spectra as a function of reaction time are shown in Figure 2. After one minute the crystalline intermediate **6** was observed, which transforms completely into compound **4** during five minutes. Full crystallization is observed after 25 min. In addition, the temperature induced phase transformation of **4** into **1** was investigated (Figure 2, right). Therefore the reaction mixture was heated up to 150 °C and **4** began to transform into **1** after 12 min. The phase transformation is already completed after 15 min.

The intermediate phase **6**, which had not been observed previously, could also be obtained by quenching the reaction mixtures. To slow down the transformation the reaction was carried out at room temperature and after 15 min the intermediate could be obtained as a phase pure product. A comparison of the EDXRD spectrum and laboratory X-ray diffraction pattern is shown in the Supporting Information, Figure S4. The intermediate phase is kinetically stable under ambient conditions (in solution as well as the isolated microcrystalline powder) (Supporting Information, Figure S4). No single crystals could therefore be obtained, and the crystal structure had to be determined and refined from powder diffraction data. The final Rietveld plot is given in Figure 3.

The crystal structure of the intermediate phase **6** is built up from two crystallographically independent copper ions (Cu1, Cu2), one completely deprotonated $(O_3P-C_2H_4-SO_3)^{3-}$ molecule, one hydroxide ion, and five water molecules. Cu1 is coordinated by six oxygen atoms through two P−O−Cu, two S−O−Cu bonds, and two hydroxide ions (O7). Cu2 is surrounded by six oxygen atoms resulting from one P−O−Cu, two S−O−Cu bonds, two water molecules (Ow1 and Ow2), and one hydroxide ion (O7). The oxygen atoms O1, O2, O3 act as end on ligands and μ-O4 and μ-O5 as bridging atoms. The copper−oxygen polyhedra form zigzag chains along the *b*-axis (Figure 4) are connected by hydrogen bonds between the sulfonate groups and water molecules (Ow3, Ow4, Ow5, Ow6) along the *c*-axis. These layers are connected by -C_2H_4- chains (Figure 4).

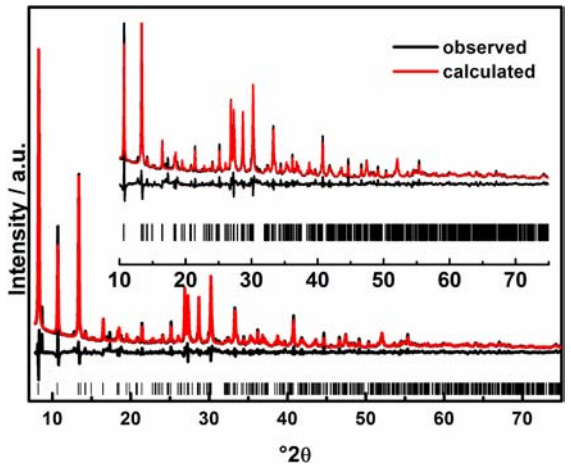

Figure 3. Final Rietveld plot of the structure refinement of **6**. The observed powder pattern is shown in black, the calculated powder pattern as an overlay in red, and the difference (observed-calculated) of both is given by the lower black line. The allowed positions of the Bragg peaks are given as tic marks.

The complete reaction pathway based on the in situ EDXRD study is shown in Figure 5. After one minute the crystalline intermediate phase is observed at 90 °C which is built up from CuO_6 polyhedra chains. One water molecule (Ow3) is located between the chains and is involved in hydrogen bonds between uncoordinated oxygen atoms (O6) from sulfonate groups and a coordinated water molecule (Ow1) (O6···Ow3 = 2.6946(5) Å and Ow3···Ow1 = 2.7876(6) Å). Upon the transformation into **4** the noncoordinating water molecule Ow3 is released and the interchain distance decreases. A new hydrogen bond network is formed between the sulfonate oxygen atom (O6) and the coordinated water molecule (Ow1). After increasing the reaction temperature to 150 °C compound **1** is formed. The coordinating water molecule (OW1) is released, and the sulfonate group completes the coordination sphere of the Cu ion.

Thermogravimetric Analysis. The thermal stability of the intermediate was investigated by thermogravimetrc (TG) analysis. The resulting TG curve is shown in Supporting Information, Figure S2. The compound shows two steps of weight loss. The first step can be assigned to the removal of six water molecules in the range of 25 to 120 °C (calc. 24.6%, obs. 26.2%), and the second step (obs. 24.0%) is due to the decomposition of the linker. The thermal decomposition leads to an X-ray amorphous residue, which contains copper and phosphorus in varying molar ratios as determined by energy dispersive X-ray analysis.

IR Spectroscopy. Compound **6** was studied by IR spectroscopy (Supporting Information, Figure S3). The broad bands between 3600 and 2900 cm^{-1} can be assigned to the uncoordinated and coordinated water molecules. The corresponding stretching vibrations appear at 1617 cm^{-1}. The bands between 1250 and 950 cm^{-1} can be assigned to the P−C, P−O, S−C, and S−O stretching vibrations of the tetrahedral CPO_3- and CSO_3-groups. Bands in the region from 3000 to 2900 cm^{-1} are due to CH_2 stretching vibrations. The corresponding CH_2-

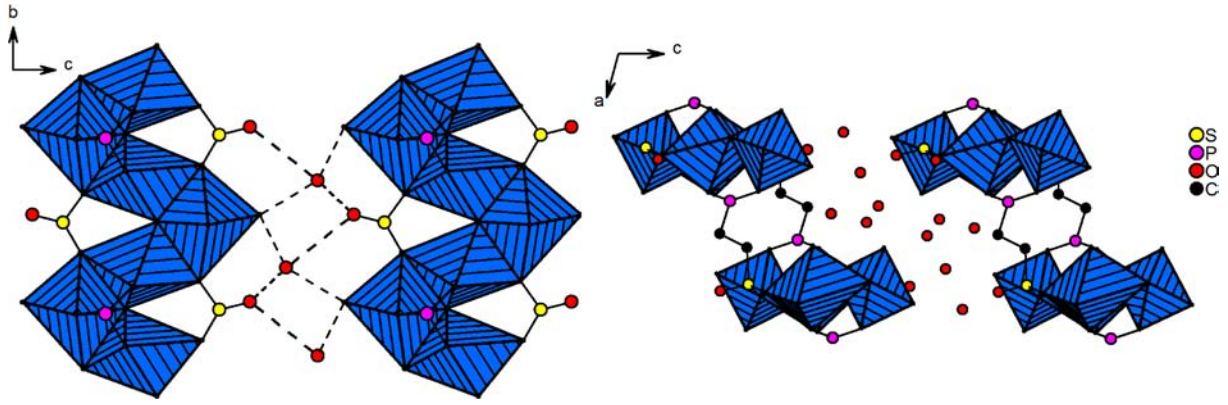

Figure 4. Crystal structure of the intermediate $Cu_2[(O_3P{-}C_2H_4{-}SO_3)(H_2O)_2(OH)]{\cdot}4H_2O$ (**6**). View along the *a*-axis (left) and the *b*-axis (right). Dashed lines represent possible H-bonds.

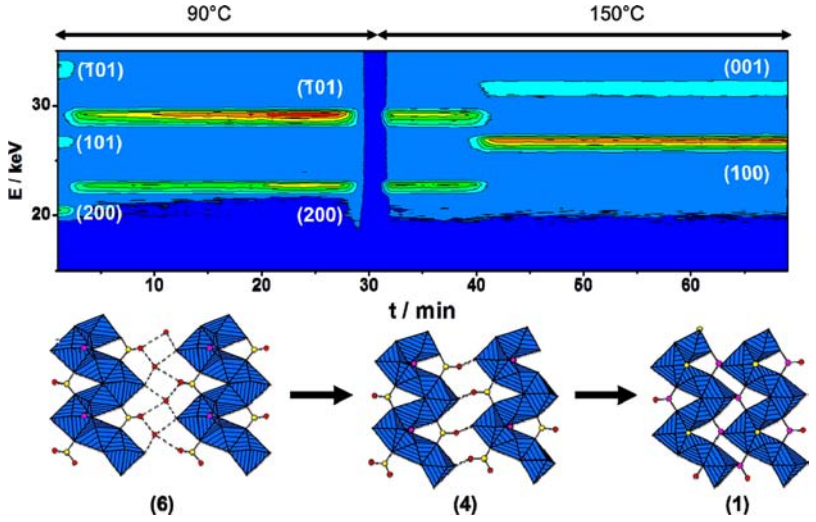

Figure 5. Illustration of the complete reaction pathway. The phase transformation at different temperatures is shown in the contour plot (top), and the correlated structural motifs of the copper oxygen chains are shown (bottom). The gap in the contour plot at ~30 min is due to the stage at which the specimen was removed from the vessel.

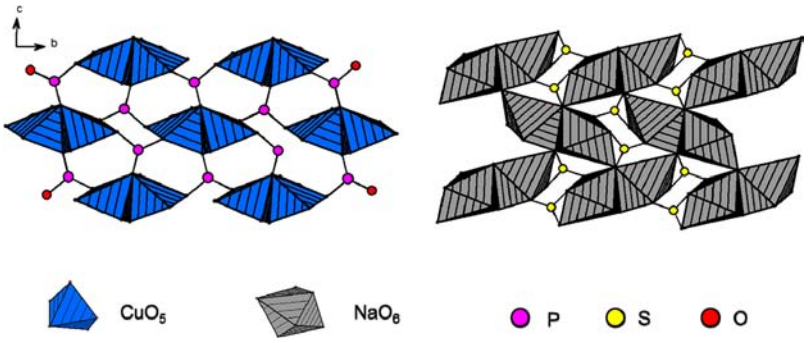

Figure 6. Section of the structure of **5**. Left: dimeric Cu_2O_8 units are connected by phosphonate groups to form layers in the *b*,*c*-plane; Right: Corner- and edge-sharing NaO_6 polyhedra are further connected by sulfonate groups to form layers in the of *b*,*c*-plane.

deformation vibration appears in the range of 1447 to 1388 cm^{-1}.

Influence of pH at a Reaction Temperature of 90 °C. The influence of the pH in the system $Cu^{2+}/H_2O_3P{-}C_2H_4{-}SO_3H/$ on the structure formation was previously only established in the temperature range 130−190 °C. No information on the structures of the phases $[Cu_{1.5}(O_3P{-}C_2H4{-}SO_3)(H_2O)]{\cdot}H_2O$ (**3**) and $NaCu(O_3P{-}C_2H_4{-}SO_3){-}(H_2O)_2$ (**5**) obtained at 90 °C were available. Therefore, two different strategies were pursued: the use of microwave assisted heating and the ligand replacement strategy which has been extensively used in the structure determination of isoreticular MOFs.[6,53−55]

Microwave-assisted heating has recently been incorporated in high-throughput methods.[18,56] To obtain suitable single crystals of $NaCu(O_3P{-}C_2H_4{-}SO_3)(H_2O)_2$ (**5**) 20 reactions were carried out, which resulted in about 50 μm large single crystals

dx.doi.org/10.1021/ic301976s | *Inorg. Chem.* 2012, 51, 12540−12547

of **5** (Supporting Information, Figure S8). These crystals were suitable for the structure determination.

Crystal Structure of $NaCu(O_3P-C_2H_4-SO_3)(H_2O)_2$ (5). The asymmetric unit is shown in the Supporting Information, Figure S7. The crystal stucture is built up from one Cu^{2+} (Cu1), one Na^+ (Na1), one completely deprotonated $(O_3P-C_2H_4-SO_3)^{3-}$, and two water molecules. Cu1 is 5-fold coordinated by four oxygen atoms through P−O−Cu bonds (O1, O2, O3) and a single water molecule (Ow1). The oxygen atoms O1 and O2 act as end-on ligand atoms and O3 as a μ-O bridging atom, which connect the CuO_5 polyhedra to edge-sharing dimers (Figure 6). These Cu−O dimers are exclusively connected via the phosphonate groups along the *c*- and *b*-axis (Figure 6, left). Na1 is 6-fold coordinated by five S−O−Na bonds (O4, O5, O6) and one water molecule (Ow2). The oxygen atoms O5, O6, and O7 act as end-on, μ-O and μ_3-O bridging atoms, respectively. The corner- and edge-sharing NaO_6 polyhedra are exclusively connected by the sulfonate groups, and layers in the *b*,*c*-plane are formed (Figure 6). Alternating layers are interconnected by the $-C_2H_4-$ organic building unit along the *a*-axis to form the final structure (Figure 7).

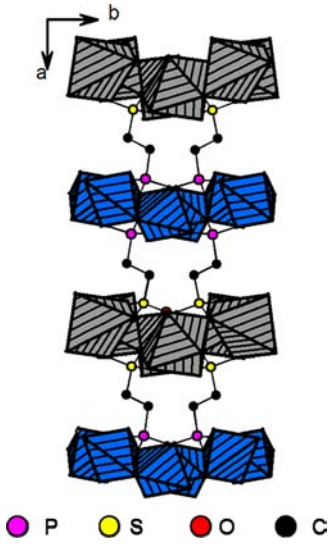

Figure 7. Section of the structure of **5**. Copper phosphonate and Sodium sulfonate layers are connected by the $-C_2H_4-$ groups (CuO_5 polyhedra blue, NaO_6 polyhedra gray).

The last of the known copper phosphonatoethylsulfonates which has not been structurally characterized so far is **3** ($[Cu_{1.5}(O_3P-C_2H_4-SO_3)(H_2O)]\cdot H_2O$). The conventional and microwave assisted synthesis of **3** led only to a microcrystalline product of intergrown needles (20 to 30 μm in lengths, Supporting Information, Figure S6). Therefore the structure had to be determined from X-ray powder diffraction data. The combination of force field calculations and Rietveld refinement allowed us to establish the crystal structure of **3**. The structural model was set up using the ligand replacement strategy.[53−55] Therefore, the powder pattern of **3** was indexed using TOPAS academic (Table 1). Comparing the lattice parameters with the ones of the previously reported compound $[Cu_{1.5}(O_3P-C_4H_8-SO_3)(H_2O)]\cdot H_2O$[52] one can expect that they form isoreticular structures (a = 5.094(2)/5.1197(5) Å, b = 8.483(2)/10.533(1) Å, c = 10.499(2)/10.800(1) Å). The difference in the *b* lattice parameter was assumed to correlate with the exchange of a $-C_4H_8-$ by a $-C_2H_4-$ group.[52] The structural model was set up using Materials Studio 5.3, and the implemented Universal Force Field (UFF) was employed for the geometry optimization. The lattice parameters were fixed to the parameters obtained by indexing. The structural model obtained was refined by Rietveld methods using TOPAS academic. The final Rietveld plot is shown in Figure 8.

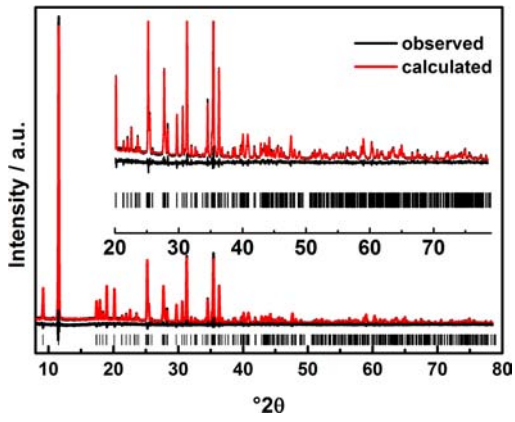

Figure 8. Final Rietveld plot of the structure refinement of compound **3**. The observed powder pattern is shown in black, the calculated powder pattern as an overlay in red, and the difference (observed-calculated) of both is given by the lower black line. The allowed positions of the Bragg peaks are given as tic marks.

Crystal Structure of $[Cu_{1.5}(O_3P-C_2H_4-SO_3)(H_2O)]\cdot H_2O$ (3). The framework contains two crystallographically independent Cu^{2+} ions (Cu1, Cu2) and one 2-phosphonatoethanesulfonate $(O_3P-C_2H_4-SO_3)^{3-}$ ion, as well as two water molecules (Ow1 coordinating and Ow2 noncoordinating). Cu1 is 6-fold coordinated by oxygen atoms through four P−O−Cu and two S−O−Cu bonds, whereas Cu2 is surrounded by five oxygen atoms through two S−O−Cu and two P−O−Cu bonds. The coordination sphere of Cu2 is completed by one coordinating water molecule (Ow1). The oxygen atoms act as end on (O1, O3, O4) as well as bridging ligand atoms (μ-O2, μ-O5), which connect the CuO_6 unit over two edges with two CuO_5 units to form Cu_3O_{12} clusters (Figure 9). These clusters are interconnected by the $-C_2H_4-$ group along the *b*-axis and by the phosphonate and sulfonate groups along the *a*-axis to form double layers, which are held together by hydrogen bonds between O6 and Ow2 (282(1) pm).

Synthesis-Structure Relationship. The structural characterization of the compounds which were obtained at 90 °C by varying the pH of the reaction mixture allows us to establish the synthesis-structure relationship.[57] The results are summarized in Figure 10. A low pH value between two and three leads to five and 6-fold coordinated face-sharing copper oxygen polyhedra. These polyhedra form isolated Cu_3O_{12} clusters which are connected by the phosphonate and sulfonate groups. Under less acidic conditions (pH = 3−7) edge-sharing zigzag chains of 6-fold coordinated CuO_6 polyhedra are found. This chain motif has already been observed for copper phosphonatosulfonates when $H_2OP-C_nH_{2n}-SO_3H$ (n = 2, 4) or *p*-$H_2OP-C_6H_4-SO_3H$ were employed.[13,43,45] Under neutral to slightly basic conditions (pH = 7−8) 5-fold coordinated copper ions are observed which form dinuclear Cu_2O_{10} clusters. The molar ratio of Cu^{2+}/Na^+ of 1:1 leads to a mixed metal phosphonatosulfonate. Sodium shows a higher affinity toward

dx.doi.org/10.1021/ic301976s | *Inorg. Chem.* 2012, 51, 12540−12547

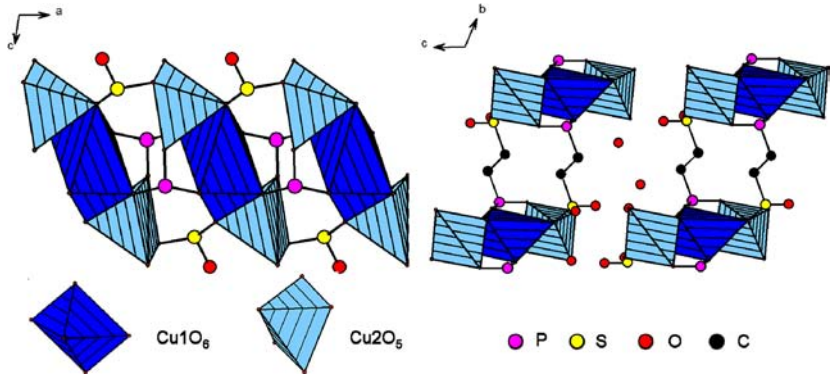

Figure 9. Sections of the crystal structure of **3**. Left: trimeric Cu−O building units are connected by sulfonate and phosphonate groups. Right: connection of the Cu phosphonate/sulfonate building units by the -C_2H_4- groups. The CuO_6 polyhedra are shown as dark blue polyhedra, and the CuO_5 are shown as light blue polyhedra.

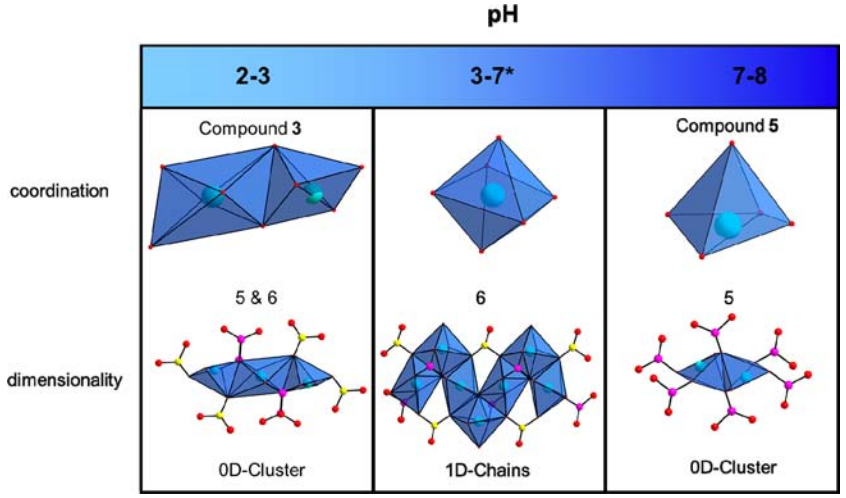

Figure 10. Influence of the pH on the coordination number and Cu−O building units formed at 90 °C (* structure reported previously).[45]

the sulfonate group and copper a higher affinity toward the phosphonate groups. Thus, a three-dimensional structure of alternating Na−O−S and Cu−O−P layers interconnected by -C_2H_4- groups was obtained. Although there is no structural data available on mixed metal phosphonatosulfonates, a few crystal structures of mixed Na/Cu phosphonates have been reported before.[58−60] Using the 7-methyl-3,11-bis-(methylphosphonic) derivate of 3,7,11,17-tetraaza-bicyclo[11.3.1]heptadeca-1(17),13,15-triene leads to selective coordination of copper to nitrogen donor atoms and sodium to phosphonate ligands.[58] The methylenediphosphonate H_2O_3P-CH_2−PO_3H_2 in combination with Na^+, Cu^{2+}, and V^{3+} leads to the coordination of all three metal species by the phosphonate group.[59] The polyfunctionalized linker HO_2C−CH_2−NH−CH_2−PO_3H_2 coordinates Cu^{2+} as well as Na^+ ions via the phosphonates group.[60]

CONCLUSION

After HT methods allowed us to establish the fields of formation of the reaction system Cu^{2+}/H_2OP-C_2H_4−SO_3H/NaOH, only the combination of in situ EDXRD measurements and alternative synthesis methods (MW-assisted heating) and advanced structure-determination methods permitted us to get a detailed view on the formation of metal phosphonates and their synthesis-structure relationships. More in situ studies on the formation of metal phosphonates should be performed, since these systems are feasible for finding crystalline intermediates that could allow a better understanding of crystallization processes.

ASSOCIATED CONTENT

Supporting Information

The asymmetric units of compound **3**, **5**, and **6**, selected bond lengths, and electron microscopic micrographs. This material is available free of charge via the Internet at http://pubs.acs.org.

AUTHOR INFORMATION

Corresponding Author

*Tel.: +49-431-880-1675. Fax: +49-431-880-1775. E-mail: stock@ac.uni-kiel.de.

Notes

The authors declare no competing financial interest.

ACKNOWLEDGMENTS

We thank the DFG (STO-643/2) for the financial support, DESY for beamtime, and Prof. Bensch (University of Kiel) and his group for the oven and the assistance at beamline F3.

REFERENCES

(1) Lee, J.; Farha, O. K.; Roberts, J.; Scheidt, K. A.; Nguyen, S. T.; Hupp, J. T. *Chem. Soc. Rev.* **2009**, *38* (5), 1450.

(2) Li, J.-R.; Kuppler, R. J.; Zhou, H.-C. *Chem. Soc. Rev.* **2009**, *38* (5), 1477.
(3) Horcajada, P.; Chalati, T.; Serre, C.; Gillet, B.; Sebrie, C.; Baati, T.; Eubank, J. F.; Heurtaux, D.; Clayette, P.; Kreuz, C.; Chang, J.-S.; Hwang, Y. K.; Marsaud, V.; Bories, P.-N.; Cynober, L.; Gil, S.; Férey, G.; Couvreur, P.; Gref, R. *Nat. Mater.* **2010**, *9* (2), 172.
(4) Rowsell, J. L. C.; Yaghi, O. M. *Microporous Mesoporous Mater.* **2004**, *73* (1−2), 3.
(5) Miller, S. R.; Pearce, G. M.; Wright, P. A.; Bonino, F.; Chavan, S.; Bordiga, S.; Margiolaki, I.; Guillou, N.; Férey, G. r.; Bourrelly, S.; Llewellyn, P. L. *J. Am. Chem. Soc.* **2008**, *130* (47), 15967.
(6) Wharmby, M. T.; Mowat, J. P. S.; Thompson, S. P.; Wright, P. A. *J. Am. Chem. Soc.* **2011**, *133* (5), 1266.
(7) Wharmby, M. T.; Miller, S. R.; Groves, J. A.; Margiolaki, I.; Ashbrook, S. E.; Wright, P. A. *Dalton Trans.* **2010**, *39* (28), 6389.
(8) Shimizu, G. K. H.; Vaidhyanathan, R.; Taylor, J. M. *Chem. Soc. Rev.* **2009**, *38* (5), 1430.
(9) Sonnauer, A.; Stock, N. *J. Solid State Chem.* **2008**, *181* (3), 473.
(10) Sonnauer, A.; Stock, N. *Acta Crystallogr., Sect. E.:Struct. Rep. Online* **2008**, *64*, M1433.
(11) Sonnauer, A.; Stock, N. *J. Solid State Chem.* **2008**, *181* (11), 3065.
(12) Sonnauer, A.; Stock, N. *Solid State Sci.* **2009**, *11* (2), 358.
(13) Maniam, P.; Nather, C.; Stock, N. *Eur. J. Inorg. Chem.* **2010**, No. 24, 3866.
(14) Du, Z. Y.; Li, X. L.; Liu, Q. Y.; Mao, J. G. *Cryst. Growth Des.* **2007**, *7* (8), 1501.
(15) Du, Z. Y.; Xu, H. B.; Mao, J. G. *Inorg. Chem.* **2006**, *45* (24), 9780.
(16) Bauer, S.; Stock, N. *Angew.Chem., Int. Ed.* **2007**, *46* (36), 6857.
(17) Feyand, M.; Nather, C.; Rothkirch, A.; Stock, N. *Inorg. Chem.* **2010**, *49* (23), 11158.
(18) Maniam, P.; Stock, N. *Inorg. Chem.* **2011**, *50* (11), 5085.
(19) Maniam, P.; Stock, N. *Acta Crystallogr., Sect. C: Cryst. Struct. Commun.* **2011**, *67*, E14.
(20) Song, J. L.; Lei, C.; Sun, Y. Q.; Mao, J. G. *J. Solid State Chem.* **2004**, *177* (7), 2557.
(21) Gemmill, W. R.; Smith, M. D.; Reisner, B. A. *J. Solid State Chem.* **2005**, *178* (9), 2658.
(22) Fredoueil, F.; Massiot, D.; Janvier, P.; Gingl, F.; Bujoli-Doeuff, M.; Evain, M.; Clearfield, A.; Bujoli, B. *Inorg. Chem.* **1999**, *38* (8), 1831.
(23) Samanamu, C. R.; Zamora, E. N.; Montchamp, J.-L.; Richards, A. F. *J. Solid State Chem.* **2008**, *181* (6), 1462.
(24) Schmidt, C.; Feyand, M.; Rothkirch, A.; Stock, N. *J. Solid State Chem.* **2012**, *188* (0), 44.
(25) Pienack, N.; Bensch, W. *Angew. Chem., Int. Ed.* **2011**, *50* (9), 2014.
(26) Surble, S.; Millange, F.; Serre, C.; Férey, G.; Walton, R. I. *Chem. Commun. (Cambridge, U. K.)* **2006**, No. 14, 1518.
(27) Shoaee, M.; Anderson, M. W.; Attfield, M. P. *Angew. Chem., Int. Ed.* **2008**, *47* (44), 8525.
(28) Hermes, S.; Witte, T.; Hikov, T.; Zacher, D.; Bahnmüller, S.; Langstein, G.; Huber, K.; Fischer, R. A. *J. Am. Chem. Soc.* **2007**, *129* (17), 5324.
(29) Juan-Alcaniz, J.; Goesten, M.; Martinez-Joaristi, A.; Stavitski, E.; Petukhov, A. V.; Gascon, J.; Kapteijn, F. *Chem. Commun. (Cambridge, U. K.)* **2011**, *47* (30), 8578.
(30) Walton, R. I.; Smith, R. I.; O'Hare, D. *Microporous Mesoporous Mater.* **2001**, *48* (1−3), 79.
(31) Millange, F.; Medina, M. I.; Guillou, N.; Férey, G.; Golden, K. M.; Walton, R. I. *Angew. Chem.* **2010**, *122* (4), 775.
(32) Millange, F.; El Osta, R.; Medina, M. E.; Walton, R. I. *CrystEngComm* **2011**, *13* (1), 103.
(33) Ahnfeldt, T.; Moellmer, J.; Guillerm, V.; Staudt, R.; Serre, C.; Stock, N. *Chem.—Eur. J.* **2011**, *17* (23), 6462.
(34) Stavitski, E.; Goesten, M.; Juan-Alcañiz, J.; Martinez-Joaristi, A.; Serra-Crespo, P.; Petukhov, A. V.; Gascon, J.; Kapteijn, F. *Angew. Chem., Int. Ed.* **2011**, *50* (41), 9624.
(35) Couck, S.; Gobechiya, E.; Kirschhock, C. E. A.; Serra-Crespo, P.; Juan-Alcañiz, J.; Martinez Joaristi, A.; Stavitski, E.; Gascon, J.; Kapteijn, F.; Baron, G. V.; Denayer, J. F. M. *ChemSusChem* **2012**, *5* (4), 740.
(36) O'Hare, D.; Evans, J. S. O.; Fogg, A.; O'Brien, S. *Polyhedron* **2000**, *19* (3), 297.
(37) Behrens, M.; Kiebach, R.; Ophey, J.; Riemenschneider, O.; Bensch, W. *Chem.—Eur. J.* **2006**, *12* (24), 6348.
(38) Kiebach, R.; Pienack, N.; Bensch, W.; Grunwaldt, J. D.; Michailovski, A.; Baiker, A.; Fox, T.; Zhou, Y.; Patzke, G. R. *Chem. Mater.* **2008**, *20* (9), 3022.
(39) Millange, F.; Serre, C.; Guillou, N.; Férey, G.; Walton, R. I. *Angew. Chem., Int. Ed.* **2008**, *47* (22), 4100.
(40) Schmidt, C.; Stock, N. *Inorg. Chem.* **2012**, *51* (5), 3108.
(41) Wragg, D. S.; Byrne, P. J.; Giriat, G. t.; Ouay, B. L.; Gyepes, R. b.; Harrison, A.; Whittaker, A. G.; Morris, R. E. *J. Phys.Chem. C* **2009**, *113* (48), 20553.
(42) Engelke, L.; Schaefer, M.; Schur, M.; Bensch, W. *Chem. Mater.* **2001**, *13* (4), 1383.
(43) Sonnauer, A.; Stock, N. *Eur. J. Inorg. Chem.* **2008**, *2008* (32), 5038.
(44) Stock, N. *Microporous Mesoporous Mater.* **2010**, *129* (3), 287.
(45) Sonnauer, A.; Lieb, A.; Stock, N. *Acta Crystallogr., Sect. E.: Struct. Rep. Online* **2008**, *64*, M1417.
(46) Wroblewski, T.; Clauß, O.; Crostack, H. A.; Ertel, A.; Fandrich, F.; Genzel, C.; Hradil, K.; Ternes, W.; Woldt, E. *Nucl. Instrum. Methods Phys. Res., Sect. A* **1999**, *428* (2−3), 570.
(47) Altomare, A.; Camalli, M.; Cuocci, C.; Giacovazzo, C.; Moliterni, A.; Rizzi, R. *J. Appl. Crystallogr.* **2009**, *42* (6), 1197.
(48) *Materials Studio*, 5.1; Accelrys: San Diego, CA, 2011.
(49) Sheldrick, G. M. *SHELXTL-PLUS Crystallographic System*; Siemens Analytical X-ray Instruments Inc.: Madison, WI, 1992.
(50) Coelho, A. *Topas Academic 4.1*; Coelho Software: Brisbane, Australia, 2007.
(51) Sabine, T. M.; Hunter, B. A.; Sabine, W. R.; Ball, C. J. *J. Appl. Crystallogr.* **1998**, *31*, 47.
(52) Sonnauer, A.; Feyand, M.; Stock, N. *Cryst. Growth Des.* **2008**, *9* (1), 586.
(53) Sonnauer, A.; Hoffmann, F.; Fröba, M.; Kienle, L.; Duppel, V.; Thommes, M.; Serre, C.; Férey, G.; Stock, N. *Angew.Chem., Int. Ed.* **2009**, *48* (21), 3791.
(54) Senkovska, I.; Hoffmann, F.; Fröba, M.; Getzschmann, J.; Böhlmann, W.; Kaskel, S. *Microporous Mesoporous Mater.* **2009**, *122* (1−3), 93.
(55) Reinsch, H.; Feyand, M.; Ahnfeldt, T.; Stock, N. *Dalton Trans.* **2012**, *41* (14), 4164.
(56) Reimer, N.; Gil, B.; Marszalek, B.; Stock, N. *CrystEngComm* **2012**, *14* (12), 4119.
(57) Forster, P. M.; Stock, N.; Cheetham, A. K. *Angew.Chem., Int. Ed.* **2005**, *44* (46), 7608.
(58) Guerra, K. P.; Delgado, R.; Lima, L. M. P.; Drew, M. G. B.; Felix, V. *Dalton Trans.* **2004**, No. 12, 1812.
(59) Yucesan, G.; Golub, V.; O'Connor, C. J.; Zubieta, J. *Inorg. Chim. Acta* **2006**, *359* (5), 1637.
(60) Clarke, E. T.; Rudolf, P. R.; Martell, A. E.; Clearfield, A. *Inorg. Chim. Acta* **1989**, *164* (1), 59.